Water Nanostructures Confined inside the Quasi-One-Dimensional Channels of LTL Zeolite

Yongjae Lee,*,† Chi-Chang Kao,‡ Sun Jin Kim,§ Hyun-Hwi Lee,|| Dong Ryeol Lee,|| Tae Joo Shin,|| and Jae-Young Choi||

Department of Earth System Sciences, Yonsei University, Seoul 120-749, Korea, National Synchrotron Light Source (NSLS), Brookhaven National Laboratory (BNL), Upton, New York 11973, Nano-Materials Research Center, Korea Institute of Science and Technology (KIST), Seoul 136-791, Korea, and Pohang Accelerator Laboratory (PAL), Pohang University of Science and Technology (POSTECH), Pohang 790-784, Korea

Received August 5, 2007. Revised Manuscript Received September 19, 2007

Understanding the formation and evolution of confined water molecules is critical in understanding many chemical and biological processes as well as the water transport inside the Earth. It is often difficult, however, to probe such processes because the host–guest interactions are dynamic in nature. Using a well-defined zeolitic channel as an ideal host and hydrostatic pressure as a driving force, we show how water molecules are introduced and evolve into various confined nanostructures up to 3.37 GPa. In the initial stage of pressure-induced hydration (PIH) occurring inside the undulating 12-ring channels of a synthetic potassium gallosilicate with zeolite LTL topology, water molecules preferentially assemble into hydrogen-bonded clusters, which alternate with water layers. With increasing PIH (by ~50%) at higher pressures, the interaction between the confined water molecules increases and the water clusters and layers are interconnected to form hydrogen-bonded water nanotubes inside the zeolitic channels. The confined water nanotube closes its maximum access diameter at further increasing pressures and gradually transforms into isolated species interacting with the zeolitic host framework. The evolution of the confined water nanostructures is well-coordinated by the concerted changes in the framework distortion and the re-entrant cation migration, which appear to be driven by the gradual "flattening" of the host 12-ring channels.

Introduction

The behavior of water in nanoconfinement is of fundamental importance.[1–3] Protein folding and pressure-induced unfolding is associated with water transport out of and into the protein interior.[4] "Water wires" or "ice nanotubes" form inside the 1D channels of SWCNs,[5,6] and novel properties, such as molecular adsorption, transport, and storage, are being discussed.[7–9] However, little is known about the mechanism of the formation and the structures of these water networks, partly because of their complex nature and difficulties in studying them. One approach to enhance our understanding is to model systems where water resides in a well-defined environment of appropriate dimensionality and periodicity, such as within the channels of aluminosilicate zeolites and other molecular sieves.[10]

Recent experimental observations of reversible and irreversible pressure-induced hydration (PIH) in zeolites with the NAT topology demonstrated how hydrostatic pressure can be used to control water content and assemble unique water structures within the confinement of the zeolitic framework.[11–13] The PIH phase of natrolite proceeds in two distinct steps: the formation of alternating single and double water bridging via 50% PIH accompanying ~7% volume expansion near 1.0 GPa, followed by the completion of helical water wires in 4_1 symmetry along the narrow elliptical 8-ring channels of natrolite upon 100% PIH above 1.2 GPa. To provide further insights into the mechanism of pressure-induced hydration and the evolution of confined water structures, in situ observation of PIH processes in a more open-channel system, if it occurs, would be necessary. We

* To whom correspondence should be addressed: Department of Earth System Sciences, Yonsei University, Seoul 120-749, Korea. Telephone: +82-2-2123-5667. Fax: +82-2-392-6527. E-mail: yongjaelee@yonsei.ac.kr.
† Yonsei University.
‡ Brookhaven National Laboratory (BNL).
§ Korea Institute of Science and Technology (KIST).
|| Pohang University of Science and Technology (POSTECH).

(1) Soper, A. K. *Physica B* **2000**, *276*, 12.
(2) Thompson, A. B. *Nature* **1992**, *358*, 295.
(3) Waghe, A.; Rasaiah, J. C.; Hummer, G. *J. Chem. Phys.* **2002**, *117* (23), 10789.
(4) Hummer, G.; Garde, S.; Garcia, A. E.; Paulaitis, M. E.; Pratt, L. R. *Proc. Natl. Acad. Sci. U.S.A.* **1998**, *95*, 1552.
(5) Hummer, G.; Rasaiah, J. C.; Noworyta, J. P. *Nature* **2001**, *414*, 188.
(6) Mashl, R. J.; Joseph, S.; Aluru, N. R.; Jakobsson, E. *Nano Lett.* **2003**, *3* (5), 589–592.
(7) Kalra, A.; Garde, S.; Hummer, G. *Proc. Natl. Acad. Sci. U.S.A.* **2003**, *100* (18), 10175.
(8) Maniwa, Y.; Matsuda, K.; Kyakuno, H.; Ogasawara, S.; Hibi, T.; Kadowaki, H.; Suzuki, S.; Achiba, Y.; Kataura, H. *Nat. Mater.* **2007**, *6*, 135.
(9) Nutzenadel, C.; Zuttel, A.; Chartouni, D.; Schlapbach, L. *Electrochem. Solid-State Lett.* **1999**, *2* (1), 30.
(10) Vaitheeswaran, S.; Yin, H.; Rasaiah, J. C.; Hummer, G. *Proc. Natl. Acad. Sci. U.S.A.* **2004**, *101* (49), 17002.
(11) Lee, Y.; Hriljac, J. A.; Parise, J. B.; Vogt, T. *Am. Mineral.* **2005**, *90* (1), 252.
(12) Lee, Y.; Vogt, T.; Hriljac, J. A.; Parise, J. B.; Artioli, G. *J. Am. Chem. Soc.* **2002**, *124* (19), 5466.
(13) Lee, Y.; Vogt, T.; Hriljac, J. A.; Parise, J. B.; Hanson, J. C.; Kim, S. J. *Nature* **2002**, *420* (6915), 485.

10.1021/cm702198x CCC: $37.00
Published on Web 11/14/2007

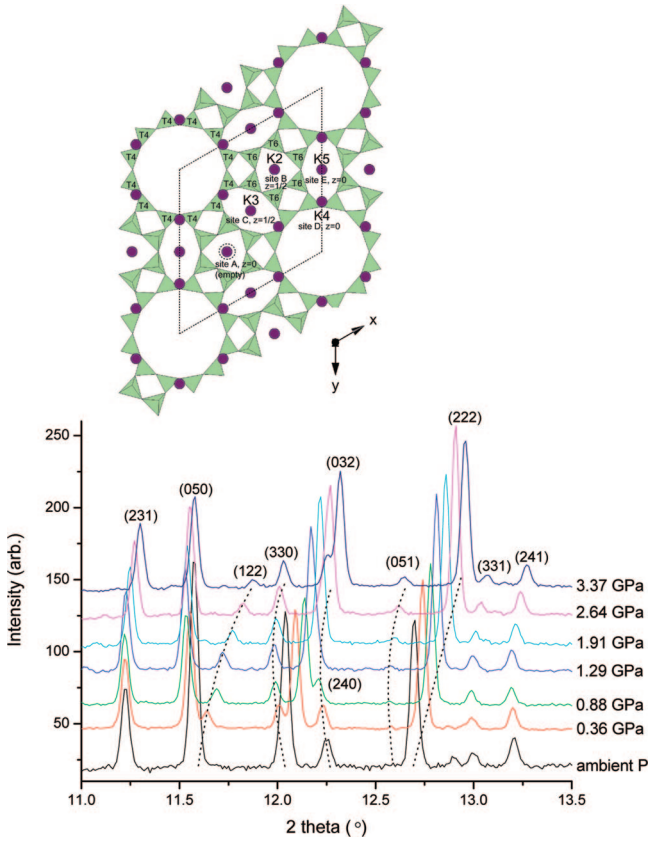

Figure 1. Details of the changes in the synchrotron X-ray powder diffraction patterns observed for K-GaSi-LTL as a function of hydrostatic pressure mediated by the alcohol and water mixture. Dotted lines are guides to the eyes to show progressive shifts in Bragg peak positions. A polyhedral representation of the K-GaSi-LTL structure is shown as an inset to emphasize the 1D channels along the *c* axis and cation positions. Water molecules that occupy the main 12-ring channels are not shown for clarity.

report here the pressure-induced growth and evolution of confined water nanostructures inside the circular 12-ring channels of a synthetic potassium gallosilicate with the zeolite LTL topology.

Zeolite LTL can be considered as one of the ideal hosts of confined water molecules because it possesses the undulating 12-ring channels, which has minimum access diameter of ca. 7 Å at the 12-ring entrance and maximum free diameter of ca. 13 Å midway between the 12-ring windows. The LTL framework is composed of the so-called cancrinite cages stacked via 6-ring windows to form columns of alternating hexagonal prisms and the cancrinite cages along the *c* axis.[14,15] These columns are connected by apical oxygen atoms of the cancrinite cages, rendering the larger circular 12-ring channels and smaller elliptical 8-ring channels along the *c* axis (Figure 1). Unlike zeolite cancrinite, the main 12-ring channel is free from stacking faults and hence has been used as an important 1D reactor in chemical reactions and reservoirs for confined host–guest syntheses.[16,17] In addition, the nonframework cations are preferentially associated with the smaller cavities and channels at the center of the cancrinite cage (site B on $z = {}^1/_2$ plane), in the middle of the elliptical 8-ring channel midway between adjacent cancrinite cages (site C on $z = {}^1/_2$ plane), and in the main channels but away from the 12-ring entrance near the recess walls of the undulating 12-ring channels (site D on $z = 0$ plane) (Figure 1). Such a partitioning of nonframework cations into the narrow cavities and channels allows for variable amounts of water molecules to form 1D clusters exclusively in the main channel system.[18]

To probe the chemical and structural evolution of confined water molecules inside the 12-ring channels, we have used monochromatic synchrotron X-ray and a high-resolution in situ gas detector. A source of external water molecules was provided by the hydrostatic pressure medium of a methanol/ethanol/water mixture in 16:3:1 ratio inside a diamond-anvil cell. Here, we show how water molecules are introduced and evolve into various confined nanostructures inside the 12-ring channels of LTL zeolite.

Experimental Section

Initial screening to find a suitable host material was conducted over several large pore zeolite samples using a symmetric diamond-anvil cell and an imaging plate detector at 5A-HFMS beamline at Pohang Accelerator Laboratory (PAL). Variable-pressure high-resolution X-ray powder diffraction measurements were performed using a Merrill-Bassett-type diamond-anvil cell and a gas-proportional position-sensitive detector (PSD)[19] at beamline X7A of the National Synchrotron Light Source (NSLS) at Brookhaven National Laboratory (BNL). A powdered sample of synthetic potassium gallosilicate LTL (ICP and TGA: $K_{12.1}Ga_{10.3}Si_{25.7}O_{72}\cdot\sim 16H_2O$) was chosen and loaded into a 300 μm diameter, 150 μm thick sample chamber in a preindented stainless-steel gasket, along with a few small ruby chips as a pressure gauge. A mixture of 16:3:1 by volume of methanol/ethanol/water was used as a pressure-transmitting fluid (hydrostatic up to ~10 GPa). The pressure at the sample was measured by detecting the shift in the R1 emission line of the included ruby chips. The sample pressure was increased in steps up to 3.4 GPa. No evidence of nonhydrostatic conditions or pressure anisotropy was detected during our experiments. The sample was equilibrated for about 30 min at each measured pressure. A monochromatic synchrotron X-ray beam of ca. 200 μm in diameter was provided by an asymmetrically cut bent Si (111) crystal. The initial sample-to-beam alignment was achieved by using a prefocused microscope, and then a 200 micron diameter pinhole was inserted to the center of the aligned sample to avoid any gasket contamination in the measured diffraction data. Diffraction data were collected for ~5 h with variable counting times [3–35° 2θ, $\lambda = 0.6482(1)$ Å], and the processed PSD data showed peak resolution of $\Delta d/d \sim 10^{-3}$, which is favorable for the structure analyses of complex materials.

The structural refinements were performed by Rietveld methods using the GSAS suite of programs[20,21] and the starting model of dehydrated gallium zeolite L by Newsam.[22] The background curve

(14) Baerlocher, C.; Barrer, R. M. *Z. Kristallogr.* **1972**, *136*, 245.
(15) Barrer, R. M.; Villiger, H. *Z. Kristallogr.* **1969**, *128*, 352.
(16) Jentoft, R. E.; Tsapatsis, M.; Davis, M. E.; Gates, B. C. *J. Catal.* **1998**, *179* (2), 565.
(17) Krueger, J. S.; Mayer, J. E.; Mallouk, T. E. *J. Am. Chem. Soc.* **1988**, *110* (24), 8232.
(18) Lee, Y.; Kim, S. J.; Ahn, D.-C.; Shin, N.-S. *Chem. Mater.* **2007**, *19* (9), 2277.
(19) Smith, G. C. *Synch. Rad. News* **1991**, *4*, 24.
(20) Larson, A. C.; VonDreele, R. B. GSAS: General Structure Analysis System, Report LAUR 86-748; Los Alamos National Laboratory, Los Alamos, NM, 1986.
(21) Toby, B. H. *J. Appl. Crystallogr.* **2001**, *34*, 210.
(22) Newsam, J. M. *Mater. Res. Bull.* **1986**, *21* (6), 661.

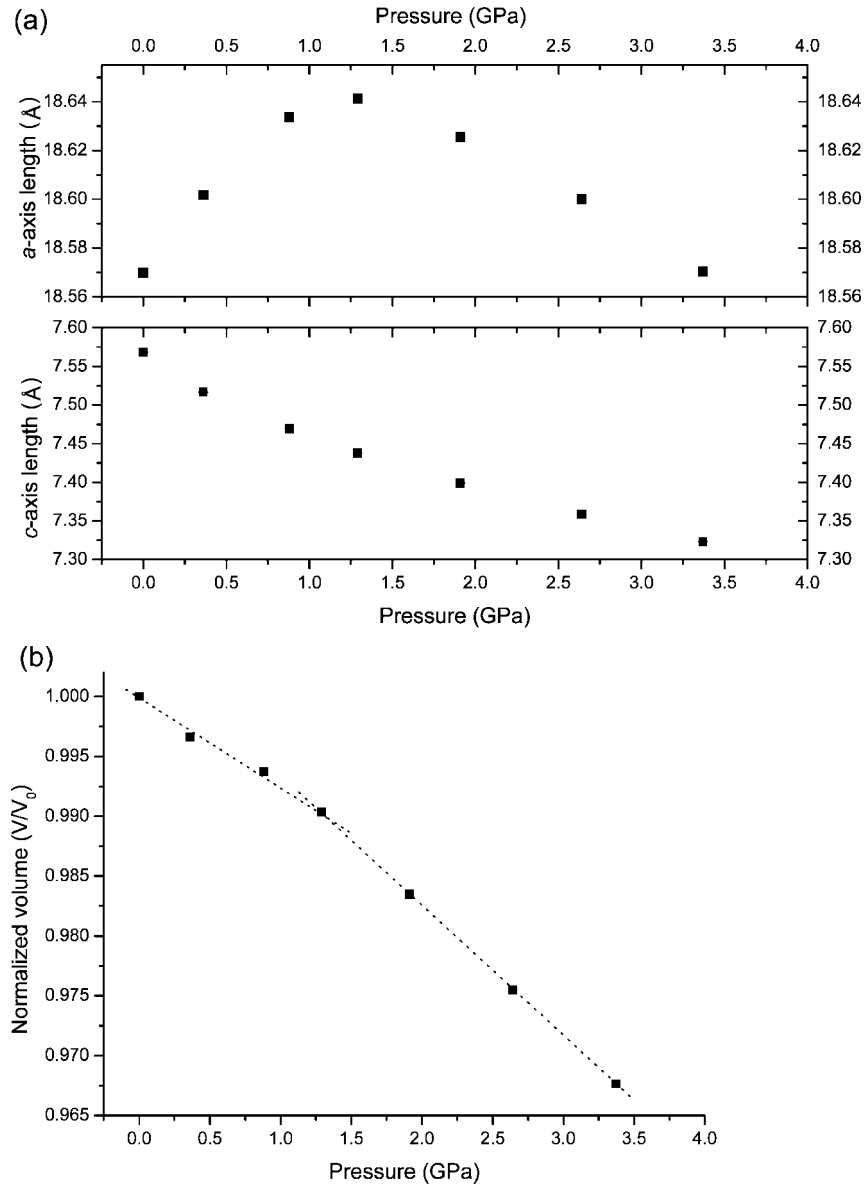

Figure 2. Changes in (a) the unit-cell edge lengths and (b) the normalized volume of K-GaSi-LTL as a function of the applied hydrostatic pressures.

was fitted by linear interpolation between selected positions. The pseudo-Voigt profile function proposed by Thompson et al.[23] was used to fit the observed peaks. To reduce the number of parameters, isotropic displacement factors were refined by grouping the framework tetrahedral atoms, the framework oxygen atoms, and the nonframework cations and water oxygen atoms, respectively. Geometrical soft restraints on the T–O (T = Ga and Si) and O–O bond distances of the tetrahedra were applied: the T–O distances were restrained to a target value of 1.663 ± 0.001 Å, and the O–O distances were restrained to a target value of 2.716 ± 0.005 Å, assuming bond lengths for Si–O and Ga–O to be 1.61 and 1.82 Å, respectively, and their random occupation and linear variations based on the measured cation ratio. Water molecules were located from difference Fourier synthesis at four or five different sites in the main channels and subsequently modeled using the oxygen scattering factor. In the final stages of the refinements, the weight of the soft restraint was reduced, which did not lead to any significant changes in the interatomic distances, and the convergence was achieved by refining simultaneously all profile parameters, scale factor, lattice constants, 2θ zero, the atomic positional and thermal displacement parameters, and occupancy factors for selected water oxygen atoms and nonframework cations. A typical Rietveld full-profile fit of K-GaSi-LTL at high pressure is shown in Supplementary Figure 1 in the Supporting Information. The final refined parameters are summarized in Supplementary Table 1 in the Supporting Information, and selected bond distances and angles are listed in Supplementary Table 2 in the Supporting Information.

(23) Thompson, P.; Cox, D. E.; Hastings, J. B. *J. Appl. Crystallogr.* **1987**, *20*, 79.

Results and Discussion

Observed changes in the diffraction patterns as a function of the applied hydrostatic pressures are emphasized in Figure 1. Visual examination of the diffraction peaks suggests that the hexagonal lattice undergoes re-entrant, anisotropic compression upon increasing pressures. Analysis of the diffraction profiles then reveals that expansion occurs in the *ab* plane up to 1.29 GPa, whereas the *c* axis contracts steadily throughout (Figure 2a), resulting in a slight change in the overall volume compression behavior (Figure 2b).

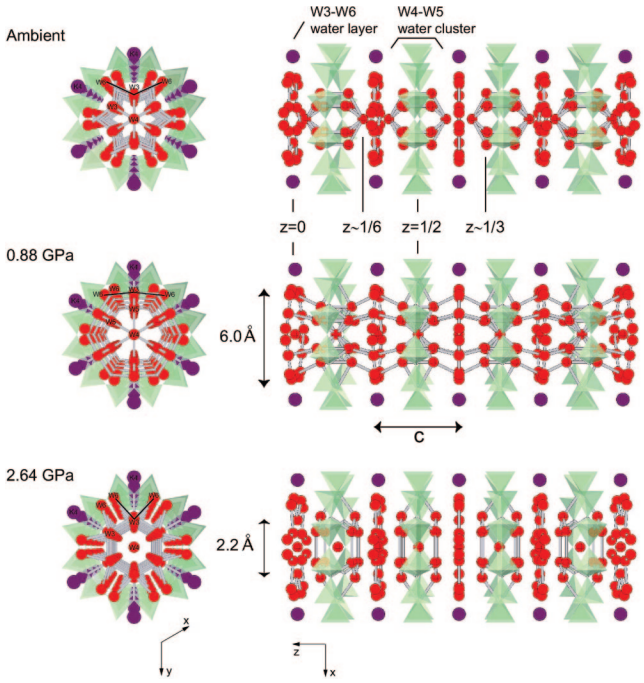

Figure 3. Evolution of confined water nanostructures formed inside the undulating 12-ring channel of K-GaSi-LTL as a function of the applied hydrostatic pressures. The 12-ring windows are shown as polyhedra, and red and purple circles represent oxygen atoms of water molecules and potassium cations, respectively. Possible hydrogen bondings are shown as bars between oxygen atoms in the range between 2.55 and 2.9 Å. Some of the K4 potassium cations are omitted in the right columns to clear the view to the water structures. The heights of the water molecules along the *c* axis are marked. Vertical arrows indicate the access openings of the water nanotubes. The puckering of W6–W3–W6 angles is emphasized in the left column. The full structural evolution derived from each measured pressure is presented in Supplementary Figure 2 in the Supporting Information.

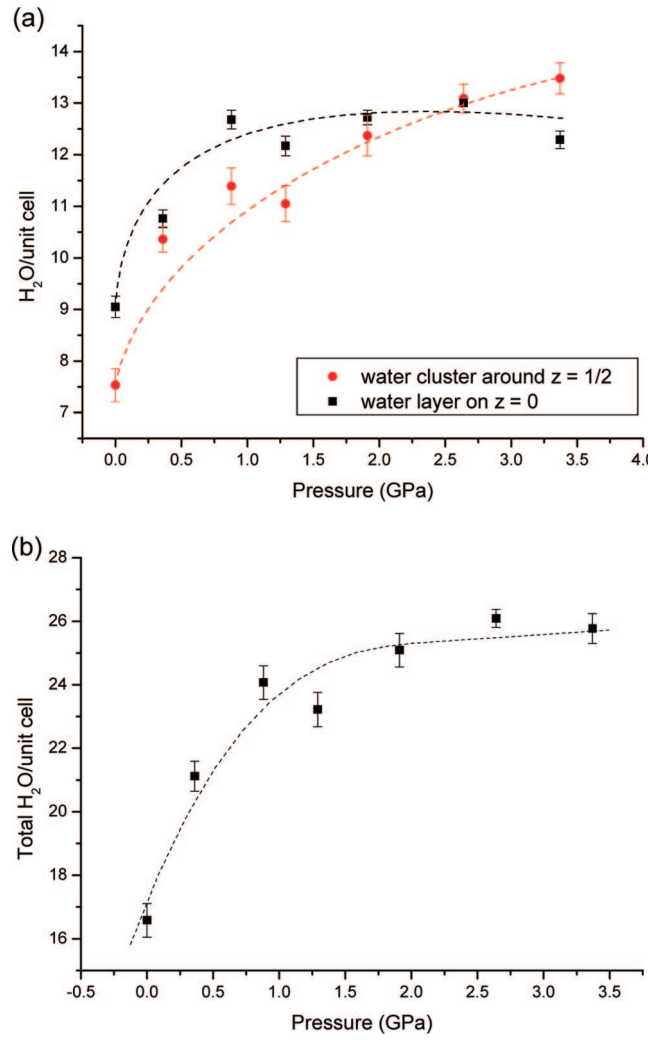

Figure 4. Pressure-induced hydration (a) occurring at the water clusters (near $z = {}^1/_2$ plane) and layers (on $z = 0$ plane) and (b) summed over a unit cell of K-GaSi-LTL. Dotted lines are guides to the eyes.

At ambient conditions, the 12-ring channels are filled by ca. 16 water molecules per unit cell (Supplementary Table 1 in the Supporting Information). The refined water positions can be approximated to $z = 0$, ${}^1/_6$, and ${}^1/_3$ planes along the channels (Figure 3). The water positions on the latter two planes (W4 and W5) separate from the other two on the $z = 0$ plane (W3 and W6) and are confined within the 12-ring windows of the main channels. Although statistically populated by water molecules, these two sites resemble a hydrogen-bonded cluster in the form of a bipyramidal hexagonal prism (Supplementary Table 2 in the Supporting Information and Figure 3). These confined water clusters are weakly held to the 12-ring window by orienting its columnar W5 oxygen atoms toward the O1 oxygen atoms of the 12-ring window. On the other hand, water molecules at the W3 and W6 sites on the wider $z = 0$ opening along the undulating 12-ring channels do not form hydrogen-bonded clusters but coordinate to potassium cations at site D near the channel walls. The water molecules in the main channel of the hydrated K-GaSi-LTL zeolite at ambient conditions thus appear to partition into two alternating groups: the more populated, hydrogen-bonded water clusters confined by the 12-ring windows and the isolated water molecules dispersed in the larger openings midway between the 12-ring windows.

As the hydrostatic pressure increases to 0.36 GPa, total refined water occupancy increases to ca. 21 water molecules per unit cell (Figure 4). A new W2 water site appears on the $z = {}^1/_2$ plane at the center of the water cluster, forming possible hydrogen bonds to the columnar W5 water molecules, with an oxygen interatomic distance of 2.84(1) Å. On the other hand, the W4 site at the apex of the bipyramidal hexagonal prism migrates with increased occupancy to the $z = 0$ plane at the center of the cation-coordinating water layer. As a result, the bonding geometry of the confined water cluster at the 12-ring window changes to a hexagonal prism (similar to the configuration of the 0.88 GPa model in Figure 3). These changes in the water content and geometry occur concomitant with the migration of the nonframework potassium cations. The partially filled K4 site starts to split into a new K5 site on the same $z = 0$ plane at the center of the elliptical 8-ring window along the *c* axis (Figure 5). This amounts to ca. 3.5 Å migration across the walls of the 12-ring channels via the boat-shaped 8-ring windows perpendicular to the *c* axis. Interestingly, this new, more symmetric coordination site has been predicted to occur when cation-coordinating water molecules are removed upon dehydration.[15] We conjecture that, in the initial stage of pressure-induced hydration, the anisotropic framework distortion drives the geometry of the 8-ring windows more energetically favorable by providing suitable square coordination environment to the new K5 cations (Figure 5).

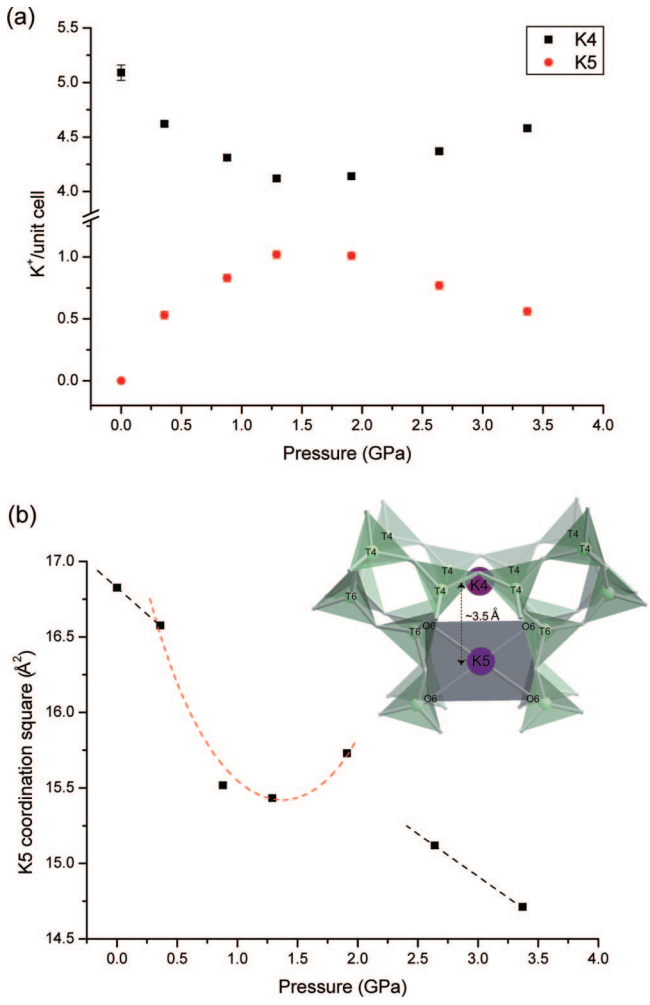

Figure 5. (a) Pressure-induced migration of potassium cations between the K4 and K5 sites and (b) concomitant changes in the potassium-coordination square defined by the four O6 framework oxygen atoms. The inset illustrates that the migration occurs across the boat-shaped 8-ring window, which forms a recess wall in the undulating 12-ring channel.

In fact, a further increase in pressure to 0.88 GPa results in continued increases in both the hydration level of water molecules to ca. 24 H_2O per unit cell and the migration of K^+ ions to the K5 site (Figures 4 and 5). At this stage, it becomes noticeable that the PIH in the main channel occurs preferentially to complete the water clusters confined by the 12-ring windows (Figure 4). It also becomes obvious that the anisotropic framework distortion leads to "flattening" of the undulating 12-ring channels in such a way to reduce the 12-ring opening and enlarge the maximum free diameter between the 12-ring windows (Figure 6). As a result, the interaction between the alternating water clusters and the cation-coordinating water layers increases and possible hydrogen bonds start to form between these two groups [Figure 3; the interoxygen distances of 2.59(3) Å between the W5 and W3 water molecules are now shown as bonds]. Although blocked by the central W2 and W4 water molecules, the resulting water column can also be described as an undulating water nanotube with alternating access diameters of 6.0 and 2.3 Å (on the basis of an oxygen ionic radius of 1.35 Å) (Figure 3).

The confined water nanotube formed at 0.88 GPa persists to 1.29 GPa, where a marginal increase in the K5 site population is observed with a slight reduction in the total refined water content to ca. 23 H_2O per unit cell (Figures 4 and 5). A further increase in pressure to 1.91 GPa then reveals that the PIH that has been occurring at the 12-ring confinement becomes saturated, whereas the PIH on the $z = 0$ plane continues to increase, leading to an overall water content of ca. 25 H_2O per unit cell (Figure 4). From this point, it seems that the major operating mechanism changes from PIH to framework distortion. This is evidenced by the observed compression behavior of the *ab* plane, or *a*-axis length, which begins to contract after reaching its maximum at 1.29 GPa (Figure 2a). Parallel to this, the changes in the geometry of the 8-ring window revert back to increase the area of the potassium coordination plane and the K5 cations begin to migrate back to the K4 site (Figure 5). There is also an indication that the interaction between the confined water molecules at the 12-ring windows decreases, as seen by the increase in the W2–W5 distance to 2.91(1) from

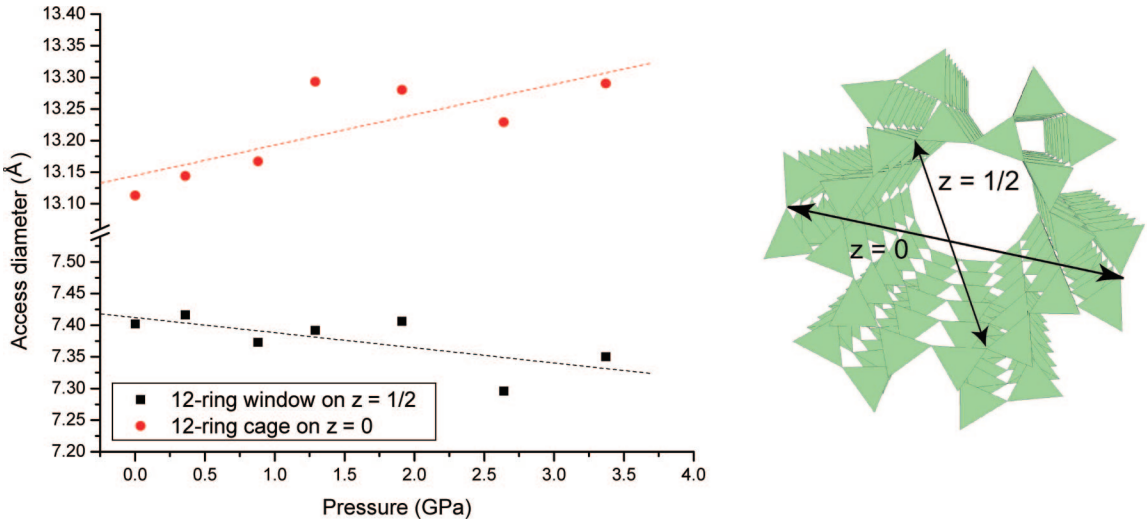

Figure 6. Pressure-induced changes in the access diameters of the undulating 12-ring channel. The "flattening" of the channel occurs by closing the 12-ring entrance on the $z = 1/2$ plane and enlarging the maximum free diameter on the $z = 0$ plane.

2.83(1) Å at 1.29 GPa (Supplementary Table 2 in the Supporting Information). This might lead to increased mobility of the central W2 and W4 water molecules inside the confined water nanotube.

The continued distortion of the host framework and the "flattening" of the undulating 12-ring channels at 2.64 GPa exert a major redistribution of the water molecules in the confined water nanotube. The decrease in the 12-ring access diameter forces water molecules at the W5 site to be pushed away from the central $z = {}^1/_2$ plane, as observed from the increase of the W5–W5 distance to 3.13(1) from 2.84(3) Å at 1.91 GPa. The increase in the maximum opening of the 12-ring channel on the $z = 0$ plane, on the other hand, induces a puckering of the water molecules on the $z = 0$ plane; the W6–W3–W6 angle decreases abruptly from 166° at 1.91 GPa to 86° at 2.64 GPa (Figure 3). This effectively transforms the geometry of the confined water nanotube to have a more uniform access diameter, similar to that of a 6-ring window, ca. 2.2 Å (Figure 3). In reality, however, it is possible that some of the water molecules might behave more like "fluid" than are located at the crystallographically fixed positions. For example, it is conceivable that the water molecules at the W3 site be statistically populated over the $z = 0$ plane because they are too close to the water molecules at the W5 site.

The structural model at the final 3.37 GPa is more or less similar to that of 2.64 GPa. The overall PIH saturates to ca. 50% level, although a marginal increase has been observed on the $z = 0$ plane since 0.88 GPa (Figure 4). The distortion of the host framework continues to drive the "flattening" of the undulating 12-ring channel (Figure 6) and the migration of the K5 potassium cations back to the K4 site (Figure 5). The separation between the water molecules at the W5 site across the $z = {}^1/_2$ plane becomes more pronounced to 3.41(1) Å. In addition, the separation between the water molecules at the W5 site *parallel to* the $z = {}^1/_2$ plane increases to 2.96(2) from 2.77(1) Å at 2.64 GPa (Supplementary Table 2 in the Supporting Information). The weakening of the interaction between these confined water molecules, however, seems to be compensated by the increased interaction to the framework. The distance between the W5 water molecules and the O1 framework oxygen atoms has decreased from 2.91(2) Å at 1.29 GPa to 2.68(2) Å at 3.37 GPa. This implies that, at further increasing pressures, the confined water nanostructures would dissociate by an increased interaction to the host framework, which might then proceed to pressure-induced amorphization.

Conclusions

We have successfully demonstrated that pressure can be used as a unique tool to create and manipulate new confined water structures inside zeolitic channels. The observed chemical and geometrical evolution of the confined water species implies corresponding changes in the storage and transport properties of the zeolitic host medium. Replacement of water molecules by other accessible molecular or monatomic species can be envisaged to synthesize noble confined guest complexes, which might possess increased stability and be recovered upon pressure release. We also conjecture that PIH could be occurring in nature under an appropriate environment, which might play an important role in the water transport to the interior of the Earth.

Acknowledgment. This work was supported by the Korea Research Foundation Grant funded by the Korean Government (MOEHRD) (KRF-2006-D00538). S. J. Kim is grateful for the support from the Korea Institute of Science and Technology (KIST). Experiments at PAL were supported in part by the Ministry of Science and Technology (MOST) of the Korean Government and the Pohang University of Science and Technology (POSTECH). Research carried out in part at the NSLS at BNL is supported by the U.S. Department of Energy, Office of Basic Energy Sciences. We gratefully acknowledge Dr. Z. Hu of the Geophysical Laboratory for access to their ruby laser system at beamline X17C.

Supporting Information Available: Supplementary Tables 1 and 2 and Supplementary Figures 1 and 2. This material is available free of charge via the Internet at http://pubs.acs.org.

CM702198X